Chimeras of Yeast and Chicken Calmodulin Demonstrate Differences in Activation Mechanisms of Target Enzymes†

Ken-ichi Nakashima, Hironobu Maekawa, and Michio Yazawa*

Division of Chemistry, Graduate School of Science, Hokkaido University, Sapporo 060, Japan

Received October 31, 1995; Revised Manuscript Received March 6, 1996⊗

ABSTRACT: Various chimeric proteins were constructed from yeast (*Saccharomyces cerevisiae*) and chicken calmodulin (CaM), and regions essential for target activation and responsible for the specific features of the yeast CaM were identified. The chimeric CaMs were designed so that each Ca^{2+} binding site of the yeast CaM was replaced in series from the C-terminus. Resulting CaM proteins showed Ca^{2+} binding properties inherent to the original Ca^{2+} binding site. Cooperative Ca^{2+} binding and a suitable rearrangement of the two EF-hand sites in each half-molecular domain were shown to be important for high-affinity interaction with CaM-dependent cyclic nucleotide phosphodiesterase (PDE). Residues in chicken CaM sequences 129−148 and 88−128, respectively, were required for low values of K_{act} (the concentration of CaM required for the half-maximal activation) in the activation of PDE and myosin light chain kinase (skMLCK and smMLCK). The difference in the structural requirements indicated different manners of the interaction. While PDE was activated to similar levels by different chimeras, the maximum activity (V_{max}) given by chicken CaMs was not achieved by any chimeric CaMs in MLCKs. Residues in chicken CaM sequences 1−50 and 88−129, in addition to Ca^{2+} binding to the fourth site, were important for high values of V_{max} of skMLCK. On the other hand, Met51 and residues in chicken CaM sequence 88−129 were critical for the high V_{max} of smMLCK. These residues may work to form the active structure of the catalytic site of each MLCK, while simple binding of CaM seems sufficient to expose the active site of PDE.

The Ca^{2+}-binding protein calmodulin (CaM)[1] is found in a variety of eukaryotic cells, and through its Ca^{2+} binding, it activates many target enzymes which are stimulated by the increase in intracellular Ca^{2+} concentration (James et al., 1995). Some 30 kinds of enzymes were proposed as targets of CaM, and CaMs isolated from vertebrates, invertebrates, plants, and protozoa show a very high degree of sequence similarity (more than 90% identical) which may be requisite for activation of many targets in the same manner (Toda et al., 1985). CaM from baker's yeast (*Saccharomyces cerevisiae*) is, however, only ∼60% identical to vertebrate CaM in the primary structure and shows characteristic properties in its function (Davis et al., 1986; Luan et al., 1987; Ohya et al., 1987). Thus, (1) yeast CaM binds only 3 mol of Ca^{2+} while others bind 4, and the set of macroscopic association constants of yeast CaM is also different from others (Luan et al., 1987; Starovasnik et al., 1993) and (2) yeast CaM is a poor activator of target enzymes from vertebrates (Luan et al., 1987; Ohya et al., 1987). In spite of these functional differences, a structure basically similar to vertebrate CaM has been proposed for yeast CaM by analyses of NMR spectra (Starovasnik et al., 1993).[2] For this reason, functional properties of yeast CaM have been studied and compared with those of vertebrate CaM to understand the target-recognition and activation mechanism of CaM (Matsuura et al., 1991, 1993; Lukas et al., 1994).

Recent NMR and X-ray analyses have revealed the structure of CaM bound to a small peptide consisting of sequences of the CaM-binding domain of myosin light chain kinases or protein kinase II (Ikura et al., 1992; Meador et al., 1992, 1993). In the complex, CaM forms a tunnel with bending of a flexible central linker portion connecting the terminal globular domains. The target peptide in the basic amphiphilic helical conformation lies in the tunnel facing its basic and hydrophobic regions to the acidic and hydrophobic region, respectively, of the inner surface of the tunnel. A wide variety of target sequences with a common basic amphiphilic helical structure can be accommodated in the tunnel with minor adjustment of the bending position, which can work as a tool for recognition of the target (Persechini & Kretsinger, 1988). Another interaction has been specified for the activation of smooth muscle MLCK (Shoemaker et al., 1990; VanBerkum & Means, 1991; Su et al., 1994). This second interaction has been suggested to be possible only after the initial interaction which induces rearrangement of the molecular surface of CaM and may work to induce the proper conformation of the catalytic site. Mutational analyses have suggested that the variable V_{max} exhibited by different CaMs can be attributed to the second interaction (Lukas et al., 1994).

† This work was supported in part by Grants-in-Aid for Scientific Research on Priority Areas 05209201 and 04225201 from the Ministry of Education, Science and Culture of Japan and by a research grant from the Naito Foundation.

* Address for correspondence: Michio Yazawa, Division of Chemistry, Graduate School of Science, Hokkaido University, Sapporo 060, Japan.

⊗ Abstract published in *Advance ACS Abstracts,* April 15, 1996.

[1] Abbreviations: CaM, calmodulin; LC2, myosin light chain 2; MOPS, 3-(*N*-morpholino)propanesulfonic acid; SDS, sodium dodecyl sulfate; PAGE, polyacrylamide gel electrophoresis; PDE, cyclic nucleotide phosphodiesterase; skMLCK, skeletal muscle myosin light chain kinase; smMLCK, smooth muscle myosin light chain kinase; N- or C-domain, the N- or C-terminal half-molecular domain of CaM each consisting of a pair of the EF-hand Ca^{2+} binding sites.

[2] S. Ohki, K. Hikichi, and M. Yazawa, unpublished results.

S0006-2960(95)02586-4 CCC: $12.00

Here, we attempted to elucidate additional aspects of the interaction of CaM with enzymes by using seven kinds of chimeric proteins from yeast and chicken CaM in which the C-terminal sequences of chicken CaM were substituted for the corresponding regions of yeast CaM. The results indicated the importance of suitable arrangement of the two EF-hand sites in the globular domains and that different targets require different regions of CaM for specific interaction.

MATERIALS AND METHODS

Molecular Cloning and Protein Engineering. Plasmids pC and pY (Matsuura et al., 1991, 1993)[3] encoding chicken and yeast CaM sequences, respectively, were used as the starting materials. Specific recognition sequences for four kinds of restriction endonucleases were first created in homologous regions of these two plamids, *Bcl*I at Leu51, *Xba*I at Ala73, *Stu*I at Ala88, and *Cla*I at Ile130, by site-directed mutagenesis using an Amersham kit (Sculuptor) and custom-synthesized oligonucleotides. Plasmids pCCC and pYYY encoding chicken and yeast CaM, respectively, contained the engineered *Stu*I and *Xba*I sites (Kimura et al., 1995). Plasmid pYYY, plasmid pYYYS129D which encodes a yeast CaM mutant containing Asp in place of Ser129, and plasmid pCCC(*Cla*I) which encodes chicken CaM contained the *Cla*I site in addition to the *Stu*I and *Xba*I sites (Matsuura et al., 1993; Kimura et al., 1995).[4] Plasmid pC-(*Bcl*I) encoding chicken CaM was created by destroying one of the two *Bcl*I sites within plasmid pC, leaving a unique site at Leu51. Plasmid pY(*Bcl*I) was constructed from pY by creating a *Bcl*I site. *Escherichia coli* strain BZ37 was used for cloning plasmids pC(*Bcl*I), pY(*Bcl*I), and others containing the *Bcl*I site to protect the site from methylation of adenine; otherwise, *E. coli* TG1 was used. *E. Coli* strain BZ37 was a gift from Dr. T. Shiba of Hokkaido University. Since each plasmid had a unique *Sca*I site derived from the vector piC10 (Inouye et al., 1986), each pair of plasmids was first double-digested with *Sca*I and one of the optional restriction enzymes (*Cla*I, *Stu*I, *Xba*I, or *Bcl*I), and product fragments that include the 5′-terminal region of the yeast CaM gene and the 3′-terminal region of the chicken CaM gene were isolated and ligated to generate expression plasmids coding chimeric CaMs YC130, YC129, YC88, YC73, and YC52 (Table 1). Expression plasmids coding chimeric CaMs YC51 and YC53 were constructed from plasmid pC1Y, which encoded YC52, by site-directed mutagenesis (see above). The nomenclature of parent plasmids, constructed expression plasmids, and expressed chimeric CaMs is summarized in Figure 1 and Table 1 together with optional restriction enzymes used for recombination.

The nucleotide sequence of the coding region within each constructed expression plasmid was verified by the dideoxy-sequencing method using *Bca*BEST (Takara).

Protein Preparation. Recombinant CaMs produced in *E. coli* TG1 were purified according to Matsuura et al. (1991) except for details in the phenyl Sepharose CL-4B column chromatography. In the purification of YCM0 and YC130, 1 M $(NH_4)_2SO_4$, which could stabilize the hydrophobic interaction, was added to the equilibration buffer containing 50 mM Tris-HCl (pH 7.5) and 0.2 mM $CaCl_2$. The concentration of $(NH_4)_2SO_4$ was decreased to 0.1 M (YCM0) or 0.2 M (YC130) in the washing buffer, and the composition of the elution buffer was the same as that of the washing buffer except for substitution of 0.5 mM EGTA for 0.2 mM $CaCl_2$. Other CaM proteins were purified using similar buffer solutions except for substitution of NaCl for $(NH_4)_2SO_4$, and concentrations of NaCl of 0.2 M in the equilibration buffer and 0.5 M in the washing and the elution buffer. EGTA was removed from CaMs by gel filtration using a Sephadex G-25 column equilibrated with 25 mM NH_4HCO_3. The purified CaMs showed a single band in polyacrylamide gel electrophoresis (Figure 2) and were stored at −20 °C after lyophilization.

Porcine brain PDE (120 kDa) was prepared according to Sharma et al. (1980) with minor modifications. A DEAE-cellulose (DE32) column was used for batches, and adsorbed proteins were eluted by 20 mM Tris/1 mM imidazole/HCl (pH 7.0), 0.15 M NaCl, 0.1 mM EGTA, 14 mM β-mercaptoethanol, and 0.1 mM PMSF. A Sephacryl S-300 column was used in the final gel filtration step.

Rabbit skeletal MLCK (65 kDa, skMLCK) and chicken gizzard MLCK (108 kDa, smMLCK) were prepared according to Nagamoto and Yagi (1984) and Yoshida and Yagi (1986), respectively. The stored sucrose powder was dissolved in a small volume of water, and the clear solution was applied to a Sephacryl S-300 column equilibrated with 20 mM Tris-HCl (pH 7.5), 0.1 M NaCl, and 14 mM β-mercaptoethanol. The second protein peak was collected and used for assay.

Gel Electrophoresis. Polyacrylamide gel electrophoresis at pH 9.4 (native PAGE) was performed according to Davis (1964) using a 15% gel. Polyacrylamide gel electrophoreses in the presence of SDS (SDS−PAGE) using a 15% gel and in the presence of 8 M urea (urea−PAGE) using a 12% gel were done according to Laemmli (1970) and Kendrick-Jones et al. (1976), respectively. After electrophoresis, proteins were stained with Coomassie brilliant blue G-250.

Ca^{2+} Binding Studies. Ca^{2+} binding to CaM was measured by the flow dialysis method using $^{45}CaCl_2$ (Du Pont-NEN) in 0.1 M NaCl and 20 mM MOPS-NaOH at pH 7.0 and 25 °C as previously described (Matsuura et al., 1993; Yazawa et al., 1992). The concentration of free Ca^{2+} in the upper cell, $[Ca^{2+}]_{free} = [Ca^{2+}]_{total}C_n/C_{T_n}$, was corrected for a consistent loss of the radioactive ligand intrinsic to our system (0.8% of $[Ca^{2+}]_{free}$ per 3 min of dialysis), as follows.

$$C_{T_n} = C_{T_{n+1}} + \alpha C_n \qquad (1)$$

where C_{T_n} and C_n are the radioactivity (counts per minute) that showed the total and free Ca^{2+} concentrations in the upper cell after the nth titration, respectively, both of which were estimated from the radioactivity in the lower cell, and α (=0.008) is the correction factor for the intrinsic Ca^{2+} loss. The concentration of Ca^{2+} bound to CaM, $[Ca^{2+}]_{bound}$, was corrected for nonspecific Ca^{2+} binding to the apparatus, which is proportional to $[Ca^{2+}]_{free}$ with a proportional constant, $\beta = 0.032$

$$[Ca^{2+}]_{bound} = [Ca^{2+}]_{bound_o} - \beta[Ca^{2+}]_{free} \qquad (2)$$

[3] Plasmids pY and pC were simply renamed here and correspond to original names pYCM0 and pCCM0, respectively.

[4] K. Tai and M. Yazawa, manuscript in preparation.

where $[Ca^{2+}]_{bound_o}$ is the observed uncorrected concentration of Ca^{2+} bound to the protein, $[Ca^{2+}]_{bound_o} = [Ca^{2+}]_{total} - [Ca^{2+}]_{free}$.

The resulting Ca^{2+} binding data were analyzed by fitting to the Adiar equation (Dixon & Webb, 1979):

$$y = (x/K_1 + 2x^2/K_1K_2 + 3x^3/K_1K_2K_3 + 4x^4/K_1K_2K_3K_4)/(1 + x/K_1 + x^2/K_1K_2 + x^3/K_1K_2K_3 + x^4/K_1K_2K_3K_4) + jx \quad (3)$$

$$y = (x/K_1 + 2x^2/K_1K_2 + 3x^3/K_1K_2K_3)/(1 + x/K_1 + x^2/K_1K_2 + x^3/K_1K_2K_3) + jx \quad (4)$$

where y is the moles of bound Ca^{2+}, x is the concentration of free Ca^{2+}, K_1-K_4 are the macroscopic dissociation constants, and j is the slope term for nonspecific binding to the protein. Equation 3 was used for CCM0, YC129, YC88, YC73, YC53, YC52, and YC51, and eq 4 was used for YCM0 and YC130.

PDE Assay. The activity was measured according to Sharma et al. (1980) in the reaction mixture (total of 400 μL) consisting of 40 mM Tris/40 mM imidazole/HCl (pH 7.0), 5 mM $Mg(OAc)_2$, 1 mM $CaCl_2$, 0.1 mg/mL bovine serum albumin, ~0.5 nM PDE, and variable amounts of each CaM in a screw-capped tube at 30 °C. To initiate the reaction, 1.2 mM cAMP was added, and after 20 min of reaction, the mixture was heated to 100 °C for 2 min to stop the reaction. After centrifugation at 3000 rpm for 10 min, 200 μL of the supernatant was withdrawn and mixed with 50 μL of 40 mM Tris-HCl (pH 7.5), 20 mM $MnCl_2$, and 1 mg/mL snake venom (*Crotalus atrox*, Sigma) to initiate the 5′-nucleotidase reaction. After 10 min of reaction at 30 °C, 35 μL of 24% SDS was added to stop the reaction. The phosphate concentration of this mixture was quantified according to Chifflet et al. (1988) and Gonzalez-Romo et al. (1992). The activation profiles shown in Figure 4 were fitted to the Hill equation (Dixon & Webb, 1979):

$$v = V_{max}[CaM]^{n_H}/(K_{act}{}^{n_H} + [CaM]^{n_H}) \quad (5)$$

where n_H, V_{max}, and K_{act} are the Hill coefficient, the maximum catalytic rate, and the concentration of CaM needed to give the half-maximal rate, respectively.

MLCK Assay. The activity was measured by the urea−PAGE method using LC2 (skMLCK) or LC20 (smMLCK) as the substrate (Matsuura et al., 1993). In some experiments, the activity of skMLCK was measured by the determination of ^{32}P incorporated into LC2 according to Corbin and Reimann (1974) as described previously (Yazawa & Yagi, 1978). In the latter method, [γ-^{32}P]ATP (10−15 cpm/pmol, Du Pont-NEN) was added to initiate the reaction at 25 °C, and 15 μL of reaction mixture was withdrawn at appropriate time intervals and spotted on filter paper (Toyo no. 50, 1 × 2 cm) which was immediately immersed in 10% trichloroacetic acid solution to stop the reaction. The radioactivity was measured with a liquid scintillation counter. The activation profiles shown in Figures 5 and 6 were fitted to the Michaelis−Menten equation (Dixon & Webb, 1979):

$$v = V_{max}[CaM]/(K_{act} + [CaM]) \quad (6)$$

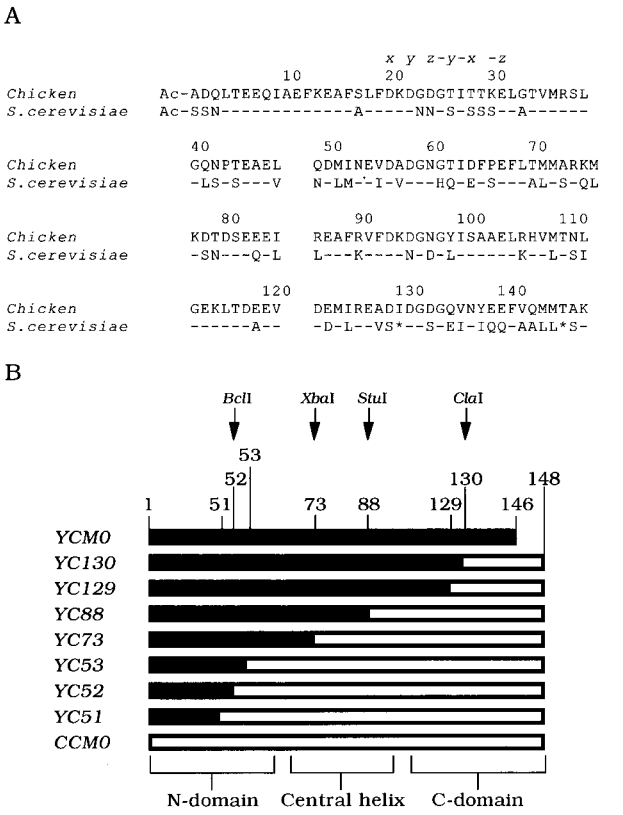

FIGURE 1: Comparison of amino acid sequences of wild-type and chimera CaMs. (A) Amino acid sequences of chicken (top) and yeast (bottom) CaM. In the sequence of yeast CaM, only substituted residues are indicated, and identical residues are indicated by dashes. Deletions at positions 130 and 146 are shown by *. Positions of the six residues coordinating to Ca^{2+} in the four EF-hand Ca^{2+} binding loops are indicated by *x*, *y*, *z*, −*y*, −*x*, and −*z*. (B) Schematic representation of sequences of chicken (open box), yeast (solid box), and chimera CaMs. Chimeric proteins were named YC*x*. In these, the N-terminal sequence of yeast CaM was ligated at position *x* (indicated in the figure) to the C-terminal sequence of chicken CaM so that the chimeric protein had a sequence of chicken CaM after position *x*. Positions of the optional sites for restriction enzymes used for recombination are shown by arrows.

where V_{max} and K_{act} are the maximum catalytic rate and the concentration of CaM giving the half-maximal rate, respectively.

Determination of Protein Concentration. The concentrations of CaM, LC2, and LC20 were determined by the biuret method (Kabat & Meyer, 1961). The concentration of enzymes was determined by the method of Bradford (1976) using a Bio-Rad protein assay reagent. Egg albumin was used as the standard.

RESULTS

To evaluate the functional contribution of each Ca^{2+} binding site and the central linker region, four kinds of chimeric CaMs were constructed with the use of four sets of unique restriction endonuclease sites which were introduced within the coding sequences of chicken and yeast CaM DNA (Figure 1, Table 1). Each of the resulting chimeric CaMs named YC*x* had a sequence of chicken CaM after residue number *x* in yeast CaM (Table 1). Some point mutations were added to these chimeric CaMs around residue number *x* to modify the length of the chicken CaM sequence, and the resulting mutant CaMs were named in a similar manner (Figure 1, Table 1).

Table 1: Summary of Construction of Plasmids and Chimeric CaMs

origin of coding sequences		optional		
yeast CaM	chicken CaM	restriction enzyme[a]	product plasmid	expressed CaM[b]
pY				YCM0
pYYY	pCCC(*Cla*I)	*Cla*I (130)	pYYY4C	YC130
pYYYS129D	pCCC(*Cla*I)	*Cla*I (130)	pYYY4CS129D	YC129
pYYY	pCCC	*Stu*I (88)	pYYC	YC88
pYYY	pCCC	*Xba*I (73)	pYCC	YC73
pY(*Bcl*I)	pC(*Bcl*I)	*Bcl*I (51)	pC1Y	YC52
			pC1Y52M	YC53
			pC1Y51M	YC51
	pC			CCM0

[a] Numbers in parentheses indicate the position in the amino acid sequence of CaM where each restriction site was introduced. [b] The chimeric CaM expressed was named YC*x*. It has a sequence of chicken CaM after residue number *x* in the yeast CaM sequence.

Bacterial Expression of Wild-Type and Chimeric CaMs. Since the *Bam*HI fragments coding the wild-type and chimeric CaMs were inserted into high-level expression plasmid piC10 (Inouye et al., 1986), each CaM protein was efficiently expressed in *E. coli* cells. The expressed CaMs were purified by hydrophobic chromatography using a phenyl Sepharose CL-4B column. All of them bound to the column stably in the presence of Ca^{2+} except for YCM0 and YC130; binding of the latter two was stabilized by addition of $(NH_4)_2SO_4$ to the equilibration buffer (Materials and Methods). A higher concentration of $(NH_4)_2SO_4$ was required for the binding of YC130 than for that of YCM0. The Ca^{2+}-dependent exposure of the hydrophobic patch may not be sufficient in the C-domain of these two proteins. Average yields were 7−15 mg of protein per liter of culture in LB medium.

Polyacrylamide Gel Electrophoresis of the Recombinant Proteins. Results of SDS−PAGE are shown in Figure 2A. All of the chimeric CaMs ran faster in the presence of 5 mM $CaCl_2$ than in its absence (5 mM EGTA), a well-known feature of CaM (Klee et al., 1979). The mobility itself and the extent of the Ca^{2+}-dependent mobility change were, however, variable. Results of the native PAGE are shown in Fgirue 2B. Here, all of the proteins migrated slower in the presence of Ca^{2+}, another feature of CaM (Grand et al., 1979). Among these proteins, YCM0 showed much slower migration both in the presence and in the absence of Ca^{2+}. All of the chimeras, including YC130, however, showed nearly the same mobility as CCM0 in the absence of Ca^{2+}. Chimera YC88 with the yeast-type central linker and YC73 with the chicken-type central linker showed similar mobility both in the presence and in the absence of Ca^{2+} (Figure 2B). Since they showed different features of Ca^{2+}-induced UV difference spectra (data not shown), conformations of their C-domains especially around Tyr138 were different. Therefore, the difference in mobility may indicate a role of the central linker region (residues 73−87) in determining the conformation of the C-domain. Chimeras YC53 and YC52 with a single amino acid substitution at residue 52 showed a considerably large difference in mobility in the presence of Ca^{2+} (Figure 2B).

Ca^{2+} Binding Ability of Recombinant CaMs. Results of Ca^{2+} binding measurements are summarized in Figure 3, and macroscopic dissociation constants obtained from the best-fit curves in Adair equation 3 or 4 (Materials and Methods)

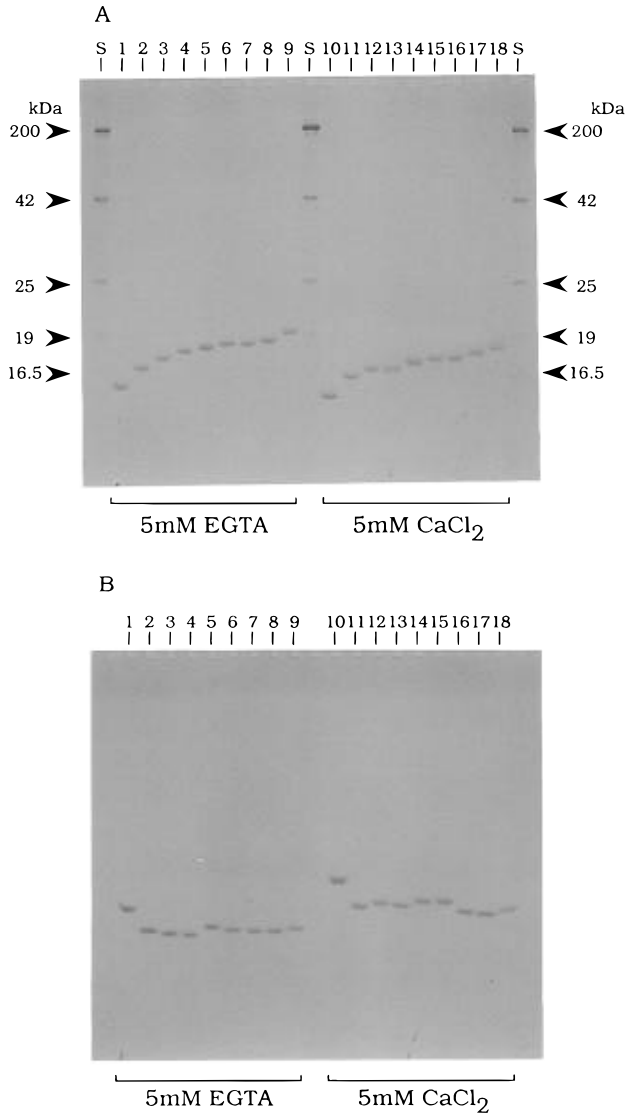

FIGURE 2: Effect of Ca^{2+} on the electrophoretic mobility of wild-type and recombinant CaMs. (A) SDS−PAGE and (B) native PAGE. In each lane, 1−2 μg of protein containing 5 mM EGTA (lanes 1−9) or 5 mM $CaCl_2$ (lanes 10−18) was applied and run on 15% gels. Samples applied to each lane were as follows: CCM0 (lanes 1 and 10), YCM0 (lanes 2 and 11), YC130 (lanes 3 and 12), YC129 (lanes 4 and 13), YC88 (lanes 5 and 14), YC73 (lanes 6 and 15), YC53 (lanes 7 and 16), YC52 (lanes 8 and 17), YC51 (lanes 9 and 18), and M_r markers (lane S).

are summarized in Table 2. Results for wild-type CaMs, YCM0 and CCM0, were similar to those reported previously (Luan et al., 1987; Starovasnik et al., 1993; Stemmer & Klee, 1994). All CaMs other than YCM0 and YC130 bound 4 mol of Ca^{2+} per mole of CaM. The maximum Ca^{2+} binding to YC130 was 3 mol/mol, while chimera YC129 with a single amino acid substitution could bind 4 mol of Ca^{2+}. In the fourth Ca^{2+} binding site of YC130, substitution of Ser129 for Asp, which is the consensus residue at the *x* ligand position of the EF-hand Ca^{2+}-binding site (Strynadka & James, 1989), may lead to the loss of Ca^{2+} binding ability. Compared to YCM0, chimeras YC130 and YC129 showed significantly lower affinity for Ca^{2+} with weaker cooperativity, especially between the second and the third Ca^{2+} bindings (Figure 3A). Chimeras YC88 and YC73, both consisting of the N-domain of yeast CaM and the C-domain of chicken CaM, showed higher cooperativity between the second and the third Ca^{2+} bindings than that of CCM0

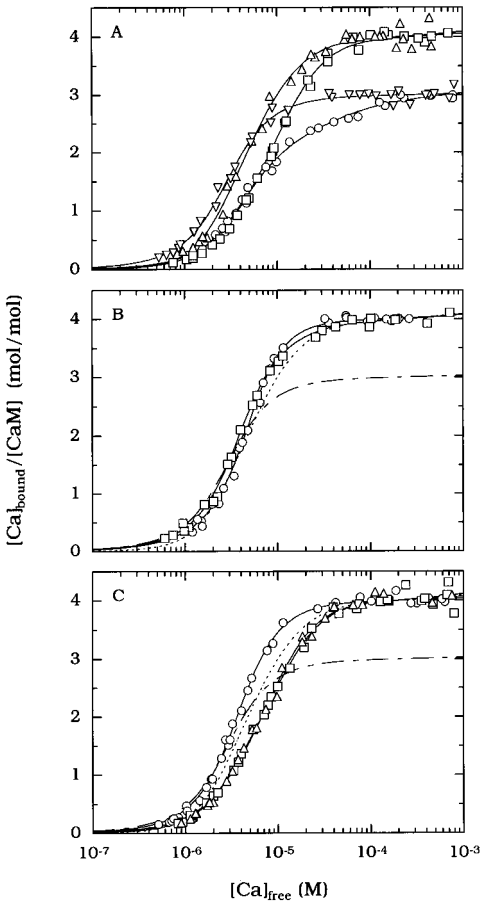

FIGURE 3: Ca^{2+} binding to mutant CaMs. Ca^{2+} binding was measured by the flow dialysis method using $^{45}CaCl_2$ in a medium of 0.1 M NaCl and 20 mM MOPS-NaOH (pH 7.0) at 25 °C. Details are shown in Materials and Methods: (A) ○, YC130; □, YC129; △, CCM0, ▽, YCM0; (B) ○, YC88; □, YC73; and (C) ○, YC53; □, YC52; △, YC51. Solid lines show the best-fit curves to Adair equation 3 or 4 for each set of data. Dotted lines and dotted broken lines in panels B and C represent Ca^{2+} binding to CCM0 and YCM0, respectively. Parameters for the best-fit curves are summarized in Table 2.

Table 2: Ca^{2+} Binding to CaM[a]

	macroscopic dissociation constants (μM)				
CaM	K_1	K_2	K_3	K_4	j
CCM0	25.2	0.336	20.6	3.71	97.7
YC51	5.55	2.45	31.9	3.70	118.9
YC52	10.3	1.10	61.7	2.63	71.7
YC53	4.01	1.95	8.78	2.29	33.9
YC73	3.16	3.50	3.80	5.60	80.4
YC88	3.66	3.39	14.4	1.58	82.3
YC129	6.29	3.20	38.9	5.00	64.4
YC130	10.9	1.53	30.4	−	63.2
YCM0	2.75	3.63	2.18	−	31.4

[a] Each set of macroscopic dissociation constants, K_1, K_2, K_3, and K_4, gives the corresponding best-fit curve to Adair equation 3 or 4 shown in Figure 3.

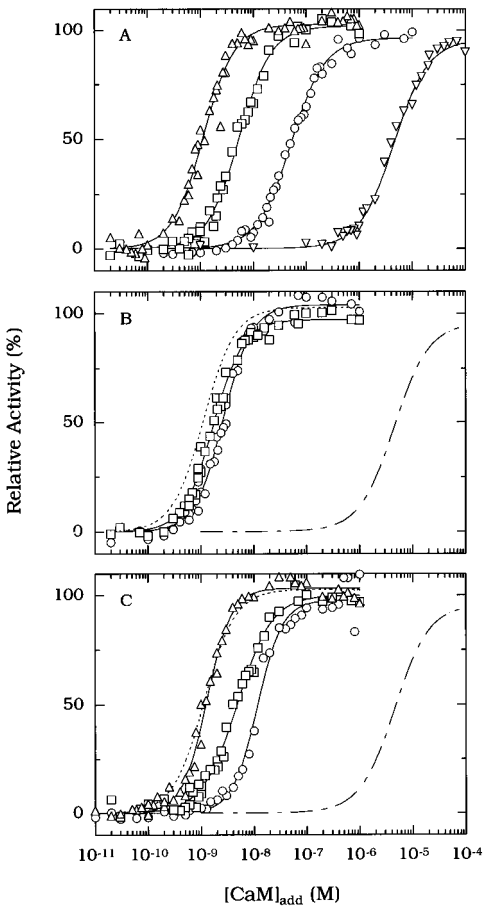

FIGURE 4: Activation of PDE by wild-type and mutant CaMs. Assay conditions are described in Materials and Methods: (A) ○, YC130; □, YC129; △, CCM0; ▽, YCM0; (B) ○, YC88; □, YC73; and (C) ○, YC53; □, YC52; △, YC51. Solid lines show the curves which fit best to the Hill equation (eq 5) for each set of data. In panels B and C, the dotted line and dotted broken line show activation curves for CCM0 and YCM0, respectively. Parameters which provide the best-fit curves are summarized in Table 3.

Table 3: Activation Parameters for PDE, skMLCK, and smMLCK[a]

	PDE			skMLCK		smMLCK	
CaM	V_{max} (%)	K_{act} (nM)	n_H	V_{max} (%)	K_{act} (nM)	V_{max} (%)	K_{act} (nM)
CCM0	103	1.14	1.5	103	2.4	105	5.1
YC51	103	1.29	1.8	88.3	6.6	99.8	35.4
YC52	100	4.81	1.3	84.2	13.9	27.5	68.1
YC53	97.7	11.6	1.8	80.0	18.3	25.1	42.9
YC73	97.2	1.74	1.5	84.2	48.6	26.9	102
YC88	104	2.71	1.6	87.0	70.0	27.1	82.6
YC129	102	5.45	1.4	53.7	3440	6.3	548
YC130	96.3	52.0	1.3	14.7	8070	5.8	7760
YCM0	95.5	4310	1.3	9.9	41300	2.3	3060

[a] Experimental results were fitted to the Hill equation (eq 5) (PDE) or the Michaelis−Menten equation (eq 6) (skMLCK and smMLCK). Each set of constants gives the corresponding best-fit curve shown in Figures 4−6.

(Figure 3B, Table 2). Three kinds of chimeras containing a heterologous mixed pair of EF-hand structures in the N-domain showed different Ca^{2+} binding properties (Figure 3C). Chimera YC53 showed a highly cooperative Ca^{2+} binding curve similar to those of YC88 and YC73, while chimeras YC52 and YC51 showed profiles similar to the one of CCM0 but with relatively lower affinity for Ca^{2+} (Figure 3C, Table 2). Met52 of yeast CaM or Ile52 of chicken CaM may have a critical role in the coupling of the two N-terminal Ca^{2+} binding sites.

Activation of Phosphodiesterase. While the V_{max} value for PDE was similar regardless of its activators (Figure 4, Table 3), the K_{act} value of YCM0 was more than 1000-fold higher than that of CCM0, which might reflect a more than 1000-fold lower affinity of YCM0 for PDE compared with that of CCM0 (Matsuura et al., 1993). Chimera YC130

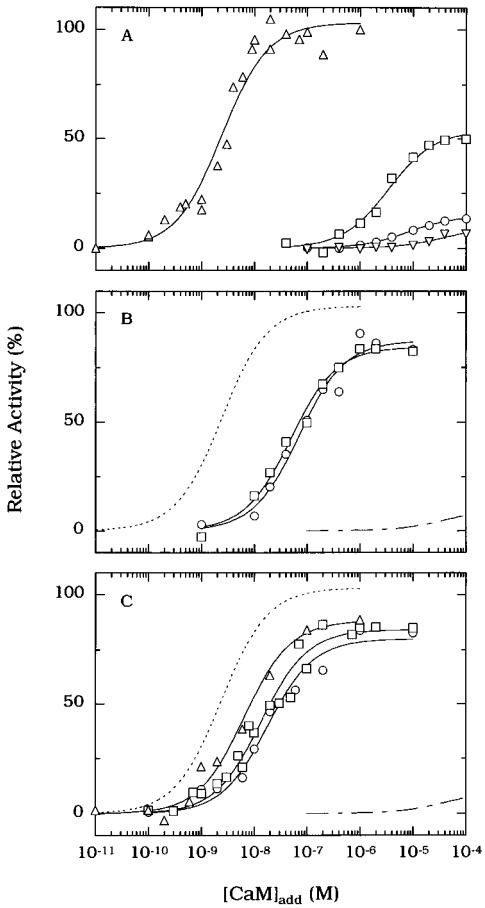

FIGURE 5: Activation of skMLCK by wild-type and mutant CaMs. Assay conditions are described in Materials and Methods: (A) ○, YC130; □, YC129; △, CCM0; ▽, YCM0; (B) ○, YC88; □, YC73; and (C) ○, YC53; □, YC52; △, YC51. Solid lines show the best-fit curves for the Michaelis−Menten equation (eq 6). In panels B and C, the dotted line and dotted broken line show activation curves for CCM0 and YCM0, respectively. Parameters which provide the best-fit curves are summarized in Table 3.

showed an 80-fold smaller value of K_{act} than YCM0 and YC129 a 9-fold greater one (Figure 4A, Table 3). With a further increase in the chicken CaM sequence to make a structure of the chicken-type C-domain, the K_{act} value of YC88 turned out to be at the same level as the value of CCM0 (Figure 4B, Table 3). We could not observe any more decrease in K_{act} in YC73 (Figure 4B, Table 3). Chimeras YC53 and YC52, consisting of heterologous structures in the N-domain, however, showed higher K_{act} values than YC73 or YC88. In these chimeras, Leu was substituted for Met51 of chicken CaM, and this might have been responsible for the higher value of K_{act}, since YC51, which had Met51, showed a K_{act} value similar to that of CCM0 (Figure 4C, Table 3).

Activation of skMLCK. YCM0 is a poor activator for skMLCK compared with CCM0 as previously described (Luan et al., 1987; Matsuura et al., 1991), and both the values of K_{act} and V_{max} were influenced variously by each activator in the present work (Figure 5, Table 3). Differences in K_{act} can be considered to reflect the different affinities for skMLCK as in the case of PDE. YCM0 showed an about 20000-fold higher value of K_{act} than CCM0 (Figure 5, Table 3), suggesting weak interaction between skMLCK and YCM0. Chimeras YC130 and YC129 showed similar high values of K_{act} (Figure 5A, Table 3), suggesting no significant site for interaction in the C-terminal sequence (residues 129−148), and Ca^{2+} binding to this sequence was not effective for the high-affinity interaction. With a further increase in the chicken CaM sequence in the C-terminal region to make the structure of the chicken-type C-domain, the K_{act} value of YC88 was 50−100-fold lower compared with those of YC130 and YC129 (Figure 5A,B, Table 3). Chimera YC73 did not show a significant difference compared with YC88 (Figure 5B, Table 3). Similarly, YC53 and YC52 showed only a small difference in the K_{act} values, ranging 2−4-fold lower than those for YC73 and YC88 (Figure 5B,C, Table 3). Chimera YC51, which had Met51 of chicken CaM, showed a small increase in the affinity compared with YC52 and YC53 (Figure 5C, Table 3), and its K_{act} value was in a range similar to that of CCM0 (Table 3).

The V_{max} value of YCM0 was about $^1/_{10}$ of the value of CCM0 (Figure 5, Table 3). Since a decrease in V_{max} can occur due to a large increase in K_m values for substrates, skMLCK activity was measured at various concentrations of substrates in the presence of YCM0 or CCM0. The time course of phosphorylation was linear for the initial 15 min in the presence of each activator, and the initial rate was determined in this range. The K_m values of skMLCK activated by CCM0 were 0.06 ± 0.01 mM and 11.6 ± 1.5 μM for ATP and LC2, respectively, and those values activated by YCM0 were 0.50 ± 0.04 mM and 35.4 ± 7.6 μM, respectively. Therefore, the effect of the substrate concentration on the observed difference in V_{max} could be excluded under our experimental conditions (2 mM ATP and 150 μM LC2), and the variable values of V_{max} can be related to the CaM-dependent creation of the catalytic site of skMLCK (Shoemaker et al., 1990; VanBerkum & Means, 1991; Su et al., 1994). Chimera YC130 showed a slightly higher V_{max} value than YCM0, but YC129 showed an about 5-fold higher V_{max} value than YCM0 and YC130 (Figure 5A, Table 3). Chimeras YC88, YC73, YC53, YC52, and YC51 showed nearly the same V_{max} value; the value was about 2.5-fold higher than that of YC129 and 80−90% of that of CCM0 (Figure 5, Table 3).

Activation of smMLCK. The activation profiles of smMLCK were similar to those of skMLCK, and both the values of K_{act} and V_{max} varied among recombinant CaMs (Figure 6, Table 3). YCM0 activated smMLCK very weakly. Compared to that of CCM0, its K_{act} was about 1000-fold higher and V_{max} was about $^1/_{50}$. Large decreases in K_{act} were observed at three steps leading to YC129, YC88, and CCM0 (Table 3). Two sequences from the chicken CaM were effective to increase the affinity as in the case of skMLCK: Asp129, which restored Ca^{2+} binding to site 4, and residues 88−128. An additional sequence, residues 1−50, was also effective for the high-affinity interaction with smMLCK. On the other hand, large increases in V_{max} were observed in chimeras YC88 and YC51 (Figure 6, Table 3). Residues in the chicken CaM sequence, Met51 and residues 88−128, which involved the linker region between site 3 and site 4, were critical to activation of smMLCK.

DISCUSSION

In this work, we constructed seven chimeric CaMs from yeast CaM and chicken CaM. Since results of NMR structural analysis on the yeast CaM suggested folding in the globular domains similar to that in vertebrate CaM (Starovasnik et al., 1993),[2] our chimeric CaMs could be

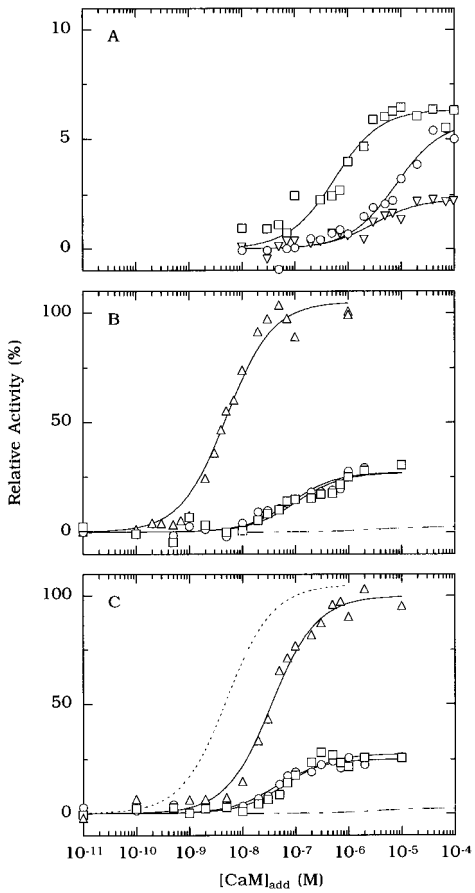

FIGURE 6: Activation of smMLCK by wild-type and chimeric CaMs. Assay conditions are described in Materials and Methods: (A) ○, YC130; □, YC129; ▽, YCM0; (B) ○, YC88; □, YC73; △, CCM0; and (C) ○, YC53; □, YC52; △, YC51. Solid lines show the best-fit curves to the Michaelis−Menten equation (eq 6). In panels B and C, the dotted line and dotted broken lines show activation curves for CCM0 and YCM0, respectively. Parameters which provide the best-fit curves are summarized in Table 3.

expected to retain the basic characteristic structure of vertebrate CaM, which might be supported by the results of gel electrophoresis (Figure 2). The similar properties of domain-exchanged chimeras YC88 and YC73, each consisting of the N-domain of yeast CaM and the C-domain of chicken CaM, strongly support the structural and functional independence of each terminal domain (Figures 3−6). But chimeras with the heterologous Ca^{2+} binding site in each half-molecular domain (YC129, YC130, YC53, YC52, and YC51) showed different properties in hydrophobic chromatography and in native PAGE (Figure 2B), suggesting some conformational difference in each domain.

Results of Ca^{2+} binding measurement could be related to the conformational difference observed by the native PAGE. Since YCM0 showed a high affinity for Ca^{2+} in a highly cooperative manner compared to YC130 or YC129 (Figure 3A, Table 2), the C-terminal sequence (residues 130−146) of yeast CaM may have a specific role to generate cooperativity among the three Ca^{2+} binding sites. Generally, the Ca^{2+} binding sites of the EF-hand make a pair to form the high-affinity Ca^{2+} binding domain (Ikura et al., 1984; Strynadka & James, 1989; Maune et al., 1992). Since the C-terminal domain of yeast CaM binds only one Ca^{2+} due to the inactive fourth site (Luan et al., 1987; Matsuura et al., 1991), the C-terminal sequence (residues 130−146) of yeast CaM may have a specific conformation in YCM0 leading to an increase in the Ca^{2+} affinity of its pair partner, which cannot be mimicked by the corresponding region of chicken CaM (Figure 3A, Table 2). The C-terminal sequence of yeast CaM might also have the ability to interact with the N-domain, and this interaction might be responsible for the observed cooperative three-Ca^{2+} binding. The low mobility of YCM0 in the native PAGE might reflect this specific structure (Figure 2).

Chimeras YC53 and YC52, both consisting of a heterologous chimeric structure of the N-domain, also showed a fairly large difference in electrophoretic mobility in the Ca^{2+}-saturated state (Figure 2B). In these mutants, an increase in mobility accompanied the decrease in Ca^{2+} affinity (Figures 2B and 3C). Since the N-domain of yeast CaM is the high-affinity site for Ca^{2+} (Starovasnik et al., 1993),[2] Met52 of the yeast CaM sequence is essential for the high-affinity coupling of the EF-hand pair and the substitution of Met52 may lead the N-domain of YC52 to the vertebrate-type low-affinity sites (Figure 3C, Table 2). According to the X-ray structure of Ca^{2+}-saturated CaM (Babu et al., 1988), the side chain of Ile52, which constitutes site 2, is observed close to the Ca^{2+} binding loop of site 1. The side chain of Met52 in yeast CaM may affect the structure of site 1, and this interaction may increase the Ca^{2+} affinity in the N-domain. If a similar mechanism is applicable to the C-domain, substitution of Leu125, a position homologous to Ile52, of chimera YC129 by Ile125 of chicken CaM may improve the Ca^{2+} affinity (Figure 3A).

The Ca^{2+} affinity of these N-domain mutants did not directly correlate to the affinity for target enzymes (Figures 3−6). Since the K_{act} value of YC73 for PDE was similar to the value of CCM0 (Table 3), the N-domain of yeast CaM was shown to recognize PDE in cooperation with the C-domain of chicken CaM. After further incorporation of the site 2 sequence of chicken CaM, the K_{act} value of YC53 increased unexpectedly. Since this chimera retained high affinity for Ca^{2+} (Figure 3C), the alignment of the four α-helical segments in the N-domain and the resulting exposed hydrophobic patch might not be suitable for the high-affinity interaction. Since this effect was improved by substitution by Ile52 of the chicken CaM sequence for Met52, the resulting chicken-type conformation of the N-domain with a concomitant low affinity for Ca^{2+} recovered the appropriate arrangement. Alignment of the four α-helices in the N-domain of yeast CaM or YC53 may result in the high-Ca^{2+} affinity-type of calbindin D_{9k} (Szebenyi et al., 1981), and the substitution for Met52 of YC53 may rearrange the structure to a type of Ca^{2+} regulatory protein like CaM (Strynadka & James, 1989). The K_{act} value was further improved by substitution of Met51 for Leu51, which restored the K_{act} value of CCM0 (Figure 5, Table 3). A possible role of Met51 was predicted by Zhang et al. (1994), and it may reflect the direct interaction of Met51 with PDE as indicated in the interaction with the skMLCK peptide (Ikura et al., 1992). The region involving Met51 and Ile52 in the N-domain and probably the homologous region in the C-domain may be very important for coupling the EF-hand pair and for the high-affinity interaction with targets.

Sequences required for high-affinity interaction with PDE, skMLCK, and smMLCK were different (Table 3). The largest increase in affinity for PDE was observed by introduction of the chicken-type C-terminal region (Asp129 to Lys148), and further small increases were observed in

YC88, YC73, and YC51 (Figure 4). In addition to the chicken CaM sequence itself (YC130), a gain of Ca^{2+} binding ability in the site 4 sequence (YC129) was also very effective for PDE (Figure 4). Therefore, residues 129−148 are the most important for high-affinity interaction with PDE (Figure 4, Table 3). A large increase in the affinity for smMLCK was similarly observed due to the restoration of Ca^{2+} binding to the fourth site (YC129). On the other hand, introduction of chicken CaM sequence Ala88 to Ala128 into mutant YC129 brought about large increases in the affinities for skMLCK and smMLCK (Figures 5 and 6). Further small increases in the affinity for skMLCK were observed by following stepwise extension of the chicken sequence (Table 3). The stepwise extension, however, did not increase the affinity for smMLCK except for an extension of the N-terminal sequence (Ala1−Asp50). The observed difference in sequences necessary for the high-affinity interaction indicated differences in the sites and the manners of interaction between CaM and the three targets. Compared to the reported molecular structure of CaM bound to various targets (Ikura et al., 1992; Meador et al., 1992, 1993), the conformation of the CaM−PDE complex may be largely different from that of the CaM−skMLCK or CaM−smMLCK complex, especially in the C-domain.

The observed differences in V_{max} may reflect another important difference in the activation mechanism between MLCKs and PDE. As different CaM mutants activated PDE to similar V_{max} levels (Figure 4), the architecture of the catalytic site of PDE might not be influenced by the activator; rather, it might simply be blocked sterically by an intramolecular inhibitory domain which is not identified yet. On the other hand, the various CaM mutants activated each MLCK to different V_{max} levels (Figures 5 and 6). Since mutations to increase the affinity for skMLCK (or to decrease K_{act}) did not necessarily increase V_{max}, our present data (Figures 5 and 6, Table 3) support the suggestion (Findley et al., 1995; Gao et al., 1993; Shoemaker et al., 1990; Su et al., 1994) that the activator of skMLCK is one of the effectors that creates a conformational alignment of the catalytic site which may directly affect the rate of phosphorylation. For skMLCK, the best conformation can be achieved through interaction with the chicken CaM sequence of residues 1−50 and 88−148, and the Ca^{2+}-saturated conformation of the C-terminal region (Asp129 to Lys148) seems most important (Figure 5, Table 3). On the other hand, Met51 and residues involved in 88−128 of the chicken CaM sequence seem critical to produce the best conformation of the catalytic site of smMLCK. Constituents around the linker of the two EF-hand Ca^{2+} binding sites in each half-molecular domain were indicated to be important for proper alignment of the catalytic site (George et al., 1990; Su & George, 1994), and the present results were consistent with their results. The essential residues indicated by George et al. (1990) and Su and George (1994) were, however, retained in YCM0, and the role of Ile52 or Ile125 in coupling the two Ca^{2+} binding sites in each domain, which was suggested in the present work, might be essential to align these residues on the molecular surface leading to the active structure of the catalytic site. Binding through Met51 to the target peptide (Ikura et al., 1992; Meador et al., 1992, 1993) would be much more important for the proper alignment of the surface residues essential for the activation of smMLCK. On the basis of these considerations, the following activation mechanisms for PDE and MLCKs are suggested. For MLCKs, CaM first binds to the enzyme, the autoinhibitory domain dissociates from the active site, and then the complete structure of the catalytic site is constructed through the second interaction of CaM with the enzyme. Then two substrates bind to start the catalytic reaction. On the other hand, PDE can be activated following simple binding of CaM, which may release the complete structure of the catalytic site, possibly through removal of the inhibitory domain.

ACKNOWLEDGMENT

We thank Professor Kazunori Sugimoto and Dr. Toshikazu Shiba for their kind gift of *E. coli* strain BZ37 and their valuable suggestions. We thank Professor Fumi Morita for valuable discussions.

REFERENCES

Babu, Y. S., Bugg, C. E., & Cook, W. J. (1988) *J. Mol. Biol. 204*, 191−204.
Bradford, M. M. (1976) *Anal. Biochem. 77*, 10−17.
Chifflet, S., Torriglia, A., Chiesa, R., & Tolosa, S. (1988) *Anal. Biochem. 168*, 1−4.
Corbin, J. D., & Reimann, E. M. (1974) *Methods Enzymol. 38*, 287−290.
Davis, B. J. (1964) *Ann. N. Y. Acad. Sci. 121*, 404−427.
Davis, T. N., Urdea, M. S., Masiarz, F. R., & Thorner, J. (1986) *Cell 47*, 423−431.
Dixon, M., & Webb, E. C. (1979) Enzymes, 3rd ed., Longman Group Ltd., London.
Findlay, W. A., Martin, S. R., Beckingham, K., & Bayley, P. M. (1995) *Biochemistry 34*, 2087−2094.
Gao, Z. H., Krebs, J., VanBerkum, M. F. A., Tang, W., Maune, J. F., Means, A. R., Stull, J. T., & Beckingham, K. (1993) *J. Biol. Chem. 268*, 20096−20104.
George, S. E., VanBerkum, M. F. A., Ono, T., Cook, R., Hanlay, R. M., Putkey, J. A., & Means, A. R. (1990) *J. Biol. Chem. 265*, 9228−9235.
Gonzalez-Romo, P., Sanchez-Nieto, S., & Gavilanes-Ruiz, M. (1992) *Anal. Biochem. 200*, 235−238.
Grand, R. J. A., Perry, S. V., & Weeks, R. A. (1979) *Biochem. J. 177*, 521−529.
Ikura, M., Hiraoki, T., Hikichi, K., Minowa, O., Yamaguchi, H., Yazawa, M., & Yagi, K. (1984) *Biochemistry 23*, 3124−3128.
Ikura, M., Clore, G. M., Gronenborn, A. M., Zhu, G., Klee, C. B., & Bax, A. (1992) *Science 256*, 632−638.
Inouye, S., Sakaki, Y., Goto, T., & Tsuji, F. I. (1986) *Biochemistry 25*, 8425−8429.
James, P., Vorherr, T., & Carafoli, E. (1995) *Trends Biochem. Sci. 20*, 38−42.
Kabat, E. A., & Mayer, M. M. (1961) *Experimental Immunology*, pp 559−560, Charles C. Thomas Publisher, Springfield, IL.
Kendrick-Jones, J., Szentkiraliyi, E. M., & Szent-Gyorgyi, A. G. (1976) *J. Mol. Biol. 104*, 747−755.
Kimura, E., Matsuura, I., Tai, K., Nakashima, K., & Yazawa, M. (1995) *Proc. Jpn. Acad. 71B*, 293−298.
Klee, C. B., Crouch, T. H., & Krinks, M. H. (1979) *Proc. Natl. Acad. Sci. U.S.A. 76*, 6270−6273.
Laemmli, U. K. (1970) *Nature 227*, 680−685.
Luan, Y., Matsuura, I., Yazawa, M., Nakamura, T., & Yagi, K. (1987) *J. Biochem. 102*, 1531−1537.
Lukas, T. J., Collinge, M., Haiech, J., & Watterson, D. M. (1994) *Biochim. Biophys. Acta 1223*, 341−347.
Matuura, I., Ishihara, K., Nakai, Y., Yazawa, M., Toda, H., & Yagi, K. (1991) *J. Biochem. 109*, 190−197.
Matuura, I., Kimura, E., Tai, K., & Yazawa, M. (1993) *J. Biol. Chem. 268*, 13267−13273.
Maune, J. F., Klee, C. B., & Beckingham, K. (1992) *J. Biol. Chem. 267*, 5286−5295.
Meador, W. E., Means, A. R., & Quiocho, F. A. (1992) *Science 257*, 1251−1255.

Meador, W. E., Means, A. R., & Quiocho, F. A. (1993) *Science 262*, 1718−1721.
Nagamoto, H., & Yagi, K. (1984) *J. Biochem. 95*, 1119−1130.
Ohya, Y., Uno, I., Ishikawa, T., & Anraku, Y. (1987) *Eur. J. Biochem. 168*, 13−19.
Persechini, A., & Kretsinger, R. H. (1988) *J. Cardiovasc. Pharmacol. 12* (Suppl. 5), S1−S12.
Putkey, J. A., Ts'ui, K. F., Tanaka, T., Lagacé, L., Stein, J. P., Lai, E. C., & Means, A. R. (1983) *J. Biol. Chem. 258*, 11864−11870.
Putkey, J. A., Slaughter, G. R., & Means, A. R. (1985) *J. Biol. Chem. 260*, 4704−4712.
Sharma, P. K., Wang, T. H., Wirch, E., & Wang, J. H. (1980) *J. Biol. chem. 255*, 5916−5923.
Shoemaker, M. O., Lau, W., Shattuck, R. L., Kwiatkowski, A. P., Matrisian, P. E., Guerra-Santos, L., Wilson, E., Lukas, T. J., VanEldick, L. J., & Watterson, D. M. (1990) *J. Cell Biol. 111*, 1107−1125.
Starovasnik, M. A., Davis, T. N., & Klevit, R. E. (1993) *Biochemistry 32*, 3261−3270.
Stemmer, P. M., & Klee, C. B. (1994) *Biochemistry 33*, 6859−6866.
Strynadka, N. C. J., & James, M. N. G. (1989) *Annu. Rev. Biochem. 58*, 951−998.
Su, Z., Fan, D., & George, S. E. (1994) *J. Biol. Chem. 269*, 16761−16765.
Szebenyi, D. M. E., Obendorf, S. K., & Moffat, K. (1981) *Nature 294*, 327−332.
VanBerkum, M. F. A., & Means, A. R. (1991) *J. Biol. Chem. 266*, 21488−21495.
Yazawa, M., & Yagi, K. (1978) *J. Biochem. 84*, 1259−1264.
Yazawa, M., Vorherr, T., James, P., Carafoli, E., & Yagi, K. (1992) *Biochemistry 31*, 3171−3176.
Yoshida, M., & Yagi, K. (1986) *J. Biochem. 99*, 1027−1036.
Zhang, M., Li, M., Wang, J. H., & Vogel, H. J. (1994) *J. Biol. Chem. 269*, 15546−15552.

BI952586L